Materials and Structures (2024) 57:178
https://doi.org/10.1617/s11527-024-02438-3

ORIGINAL ARTICLE

Effects of exposure sequence and GGBS cement replacement on performance of concrete subjected to carbonation and chloride ingress

Grace A. Blackshaw · Jessica C. Forsdyke · Janet M. Lees

Received: 8 September 2023 / Accepted: 13 July 2024

Abstract In a variety of applications, such as in tidal zones, abutments of bridges and concrete tunnel linings, reinforced concrete is exposed to both carbonation and chloride ingress. The exposure can be either simultaneous or sequential. However, durability design rarely considers synergistic effects due to carbonation and chloride ingress, even though this may have detrimental consequences for performance. Comparative implications of exposure sequence across different concrete compositions are also unknown. In this study, an experimental investigation on the effects of the sequence of carbonation and chloride ingress was conducted, using two concretes which differ by 50% cement replacement with ground granulated blast furnace slag (GGBS). Specimens were exposed to a combination of 10% CO_2 accelerated carbonation and immersion in 3% sodium chloride solution, in either sequence, and compared with companion samples subjected to only one of these aggressive environments. The extent of carbonation was measured using phenolphthalein indicator solution, while silver nitrate and Rapid Chloride Testing provided indicators of the chloride ingress. For both concrete mixes, specimens with prior chloride ingress exhibited a decreased rate of carbonation when compared to specimens with no prior exposure. Conversely, specimens with prior carbonation displayed an increased rate of chloride ingress compared to non-carbonated counterparts and a step in the acid soluble chloride content in the region of the carbonation front. The concrete composition appeared to play a role since a greater increase in chloride diffusion coefficient due to prior carbonation was observed in the mix with 50% GGBS replacement than the mix without. These findings suggest that in concrete structures exposed to air and saline environments, the effects of sequential exposure should be characterised.

Keywords Concrete · Carbonation · Chloride ingress · Exposure sequence · GGBS

1 Introduction

Concrete is the most commonly used material in construction, largely due its low cost, versatility, excellent resistance to water and the wide-spread availability of its primary components [1]. Understanding the durability performance of reinforced concrete is important because the deterioration of concrete infrastructure has significant safety, cost, and environmental implications [2–6]. Implications for ordinary Portland cement (OPC) cementitious binders with supplementary cementitious material (SCM) replacement such as ground granulated blast furnace slag (GGBS) also require further elucidation as such

G. A. Blackshaw · J. C. Forsdyke · J. M. Lees (✉)
Department of Engineering, University of Cambridge, Cambridge, UK
e-mail: jml1010@cam.ac.uk

Published online: 10 September 2024

materials have different chemical compositions and particle distributions [7, 8].

In a variety of circumstances, such as in marine environments, bridge abutments and concrete tunnels, concrete is exposed to both carbonation and chloride ingress either simultaneously, in succession, or cyclically [9]. Durability design rarely considers the combined effect of carbonation and chloride ingress [10]. In certain cases, consideration of degradation mechanisms independently has been found to overestimate the durability performance of concrete [4, 10].

Simultaneous exposure to carbonation and chloride ingress has been previously considered [11–13]. However, sequential exposure can be more readily implemented using conventional laboratory equipment so is more common in existing studies. In such studies, there is broad agreement that chloride exposure after prior carbonation increases the apparent chloride diffusivity of OPC binders [4, 6, 14–16]. Ngala and Page [17] carried out pore size distribution studies on carbonated and non-carbonated OPC and GGBS pastes and found there was a reduction in the total porosity due to carbonation, which potentially reduces the chloride diffusivity, but an increase in the proportion of large capillary pores, which could contribute to an increase in chloride diffusivity. It was postulated that the reduction in total pore volume could be due to deposition of $CaCO_3$ during carbonation, as the volume of $CaCO_3$ is greater than the volume of the hydrates, and that the pore coarsening was associated with the formation of additional silica gel due to the decomposition of C–S–H gel during carbonation [17]. Ngala and Page [17] also found that for fully carbonated OPC and GGBS pastes the chloride diffusion rates depended primarily on physical mechanisms and were not significantly affected by ion-pore surface interactions [17]. Chang [18] found that complete carbonation reduced the chloride binding capacity of OPC and GGBS pastes to approximately zero. It is suggested that the AFm phases (alumina, ferric oxide and monosulfate, please see [19] for phase details) react with carbonate ions to form monocarboaluminate phases, thereby depleting the AFm availability for reactions with chloride ions to form Friedel's salt, and because the C–S–H gel is carbonated there is then no more C–S–H gel to absorb chloride ions [18]. Ye et al. [20] investigated chloride ingress in OPC samples and samples with fly ash and GGBS replacement exposed to cyclic drying-wetting and carbonation and found carbonation to have a significant impact on the distribution of free chloride. The free chloride content at the surface dropped and the chloride content reached a maximum 7–9 mm into the sample, which likely coincided with the carbonation front [20]. It is suggested that the reduced pH value of concrete pore solution due to carbonation increases the solubility of Friedel's salt, leading to a chloride gradient and thus facilitating the inward movement of chloride ions [20]. The pore size distribution carried out by Ye et al. [20] shows a similar reduction in porosity and increase in average pore size to that reported by Ngala and Page [17], which Ye et al. suggest could be responsible for the reduction in chloride content in the carbonated region of concrete. Liu et al. [21] investigated the impact of prior carbonation on chloride ingress due to chloride aerosol exposure in OPC concrete and found a similar reduction in the free chloride content at the surface and increase in the length of the convection zone to that observed by Ye et al. [20]. SEM micrographs from Liu et al. [21] show a more compact structure for the sample exposed to prior carbonation and chloride aerosol, compared to a more fractured structure for the sample exposed to just chloride aerosol. Liu et al. [21] found a reduction in porosity due to carbonation, but, unlike Ye et al. [20] and Ngala and Page [17], found an increase in the proportion of smaller capillary pores due to carbonation.

Research on the impact of prior chloride on carbonation is more limited [10, 21–23]. Although there is general agreement that prior chloride exposure reduces the rate of carbonation in OPC, the materials and exposure conditions studied vary significantly. Kuosa et al. [10] found that carbonation was minimal when concrete specimens with various binder types first underwent a rapid chloride migration test (RCMT). Malheiro et al. [22] found that prior chloride exposure reduced the carbonation depth in OPC mortars. Lui et al. [21] found that prior chloride aerosol exposure led to reduced carbonation depths in OPC concrete. It is suggested that the ability of salt to physically block the pores of the cement matrix contributes to this reduction in carbonation with prior chloride ingress [23]. Optical images from Malheiro et al. [22] show a crystalline structure in the pores of OPC mortars subjected to prior chloride exposure and carbonation, supporting this hypothesis. It is suggested that the hygroscopic nature of salt, which

increases the moisture content and water film thickness inside the pores, also contributes to the reduction in carbonation [22]. Malheiro et al. [23] carried out immersion water absorption tests in OPC concrete and found a reduction in porosity for specimens immersed in chloride and then exposed to carbonation, compared to specimens only exposed to carbonation. Lui et al. [21] found a similar reduction in total porosity, along with a reduction in the proportion of medium and large capillary pores, under chloride aerosol exposure and carbonation.

OPC replacement with GGBS has generally been found to increase the rate of carbonation [24–27]. It is believed that this is due to the consumption of portlandite during the hydration of GGBS, which decreases the alkalinity of the cement paste, resulting in more rapid carbonation [24]. In contrast, cement replacement with GGBS has been found to reduce rates of chloride ingress relative to OPC binders [17, 24, 28, 29]. Rates of chloride ingress in concrete are generally affected by the concrete's permeability and the chloride binding capacity of its cement matrix [29]. The refined pore structure of cement pastes with GGBS replacement reduces their permeability [24]. Chloride binding occurs when chlorides react chemically with tricalcium aluminate (C_3A) to form Friedel's salt [29]. Thermal analysis measurements carried out by Dhir et al. [29] suggest that the increased aluminate content of GGBS is largely responsible for its improved chloride binding capacity [29]. Abd El-Fattah et al. [30] suggest that the increased calcium and aluminate content of GGBS both contribute to its improved chloride binding capacity. There is also evidence of the adsorption of chloride ions on the surface of C–S–H, but this is less well understood [29, 31]. Limited research exists on the impact of GGBS replacement on sequential carbonation prior to chloride ingress or chloride ingress prior to carbonation. Ngala and Page [17] found that the increase in capillary porosity and in the proportion of large capillary pores due to carbonation was greater for pastes containing GGBS than for pure OPC pastes. It is suggested that the hydraulicity of GGBS reduces the amount of portlandite, producing additional C–S–H gel that can be decomposed to form silica gel [17]. These different phenomena are likely to influence carbonation, chloride diffusion and chloride distribution in OPC/GGBS concrete subjected to sequential exposure.

In the current work, chloride ingress prior to carbonation or carbonation prior to chloride ingress are investigated using an OPC and a 50% OPC/50% GGBS concrete such that direct comparisons can be made. The main objectives are to investigate: the effect of exposure sequence on concrete subjected to carbonation and chloride; the role of GGBS replacement on the observed behaviour; and the applicability of single exposure carbonation or chloride ingress models for concretes with existing carbonated or chloride fronts. Cases where consideration of carbonation or chloride diffusion ingress independently could over-estimate the durability performance are discussed. The results thus inform guidance for the long-term integrity of reinforced concrete structures exposed to carbonation and chloride ingress.

2 Experimental justification and investigation

The experimental approach combines accelerated carbonation and chloride immersion of selected concrete mixes. The exposure conditions, concrete mix compositions, and experimental procedures are presented.

2.1 Carbonation and chloride exposure conditions

Naturally, carbonation is a slow process due to an atmospheric CO_2 concentration of approximately 0.04% [32]. Atlantic seawater has a 3% Cl concentration [33]. Even after only a month or two, full submersion in 3% sodium chloride solution for chloride ingress exposure is likely to lead to measurable chloride fronts (> 5 mm) beyond the surface layer in most concretes. However, this is not the case for 0.04% carbonation exposure ingress as the carbonation ingress is slower and progression front times longer. Therefore, carbonation was accelerated by containment in a controlled CO_2 environment.

One concern with accelerated testing is that different concrete compounds carbonate at different CO_2 concentrations [34]. Cui et al. [35] found that Ordinary Portland cement concrete samples exposed to CO_2 concentrations greater than 20% formed a dense carbonated concrete microstructure in the outermost layer of concrete, which reduced the rate of CO_2 diffusion. This was not the case for concrete samples exposed to lower CO_2 concentrations (below 20%). This led to a choice of a 10% CO_2 concentration. In

the case of the prior carbonation experimental specimens, the depth of the carbonation front will be deeper than it would be in practical applications at the time of chloride exposure. However, the beneficial trade off was that in the specimens with prior chloride exposure, accelerated carbonation allowed more scope for the carbonation front to pass through the chloride front.

2.2 Materials and mix selection

Two concrete mixes were selected, to enable exploration of the impact of cement replacement with GGBS on durability performance under sequential exposure. These are referred to as C100 and C50G50, based on the proportion of binder which was CEM II/A-LL cement (C) or GGBS slag (G). The mix proportions are shown in Table 1. C100 was designed using the BRE mix design method for normal concrete mixes [36], with 100% CEM II/A-LL 32.5 R cement as the binder, and a *w/b* ratio of 0.7. A high water/binder ratio was chosen to ensure that significant carbonation and chloride ingress occurred within the proposed timeframe and to observe phenomenological trends. However, it should be noted that such a high *w/b* ratio is unlikely to be used in practice. The composition of C50G50 was identical to that of C100, except that 50% by mass of the binder was replaced with GGBS. Such replacement proportion is typical in practice to maximise carbon dioxide emissions savings, while maintaining adequate cementitious activity [37]. The specific gravities of OPC and GGBS have been found elsewhere to be 3.1 g/cm^3 and 2.87 g/cm^3 [38] so a volume equivalence mix design would have led to a slightly different mass of GGBS than what was used here.

2.3 Casting and curing

Four 100 mm × 100 mm × 500 mm concrete prisms were cast from each mix in accordance with EN 12390-2:2019 [39]. As sawn surfaces were required for chloride ingress, the concrete prisms were subsequently cut using a diamond wet-cut saw into five 100 mm × 100 mm × 100 mm cubes, resulting in a total of 20 cubes per mix. This also ensured identical casting and curing treatment of specimens which would later be exposed to carbonation or chloride ingress. Additionally, companion 100 mm × 100 mm × 100 mm concrete cubes were cast for compressive strength tests. The concrete was placed roughly in thirds and vibrated using a vibrating table. The slump of mix C100 was recorded as 65 mm whereas the slump of mix C50G50 was 15 mm. After 7 days of curing in a water bath at 20 °C, the prisms were cut into cubes, and held in laboratory conditions (20 °C and 50% relative humidity) for a further 23 days until aged 30 days.

The cubes for compressive strength tests were cured in a water tank until testing, in accordance with BS EN 12390-3 [40]. The compressive cube strengths were measured at 7, 28 and 64 days, following the protocol of BS EN 12390-3 [40].

2.4 Experimental programme

After curing, cubes with sawn faces were exposed to a sequential combination of carbonation and chloride ingress in phases 1 and 2 ($35Cl + tCO_2$ or $35CO_2 + tCl$) as summarised in Table 2. Comparator cubes to be subjected to a single exposure condition in phase 2 ($35 + tCO_2$ and $35 + tCl$) were stored in sealed plastic bags under controlled conditions such that they were the same age as the specimens undergoing dual exposure with prior carbonation or chloride ingress during phase 1. The total duration, *t*, of phase 2 exposure was 35 days. Therefore, the final measurements were taken 100 days after the concrete was initially cast.

Table 1 Concrete mix constituents and proportions

	CEMII/A-LL cement (kg/m^3)	GGBS (kg/m^3)	0–10 mm gravel (kg/m^3)	0–4 mm sand (kg/m^3)	Water (kg/m^3)	Water/binder ratio
C100	286	0	1021	740	200	0.70
C50G50	143	143	1021	740	200	0.70

Table 2 Summary of the exposure sequence and exposure notation

Exposure notation	Phase 1 exposure	Transition period	Phase 2 exposure
$35+t\mathrm{CO_2}$	None (sealed), 34 days	1 day	Carbonation, *t* days
$35+t\mathrm{Cl}$	None (sealed), 34 days	1 day	Chloride, *t* days
$35\mathrm{Cl}+t\mathrm{CO_2}$	Chloride, 34 days	1 day	Carbonation, *t* days
$35\mathrm{CO_2}+t\mathrm{Cl}$	Carbonation, 34 days	1 day	Chloride, *t* days

2.5 Carbonation conditions and preparation

Before commencing carbonation exposure, five of the six sides of the cubes were sealed with vinyl tape, leaving one sawn face exposed. The conditions in the carbonation chamber were 10% CO_2, 20 °C and 55% relative humidity. After carbonation exposure, the cube specimens were split using a tensile splitting test apparatus. Phenolphthalein (Ph) indication was used to visually identify the carbonation penetration depth [41]. The freshly split surfaces were sprayed with 1% phenolphthalein in ethanol solution and left for 1 h for the colours to develop prior to measurement of the carbonation depth.

For the $35\mathrm{Cl}+t\mathrm{CO_2}$ specimens exposed to chloride solution prior to carbonation, the cubes were removed from the solution, oven dried for 3 h at 30 °C, air dried for a further 33 h, rewrapped in vinyl tape, and then placed in the carbonation chamber with a controlled relative humidity of 55%. Although the internal moisture conditions at the onset of carbonation exposure were unknown, there was consistency in the methodology for both the OPC and OPC/GGBS specimens.

2.6 Chloride ingress conditions and preparation

Cubes were prepared for chloride ingress by vacuum saturation according to BS EN 12390-11:2015 [33]. Five of the six sides of the cubes were then sealed with vinyl tape, leaving one sawn face exposed. After sealing, the cubes were placed in saturated calcium hydroxide solution for 18 h, then transferred directly to a container containing 3% sodium chloride solution at 20 °C, and the container sealed. For the cubes with prior carbonation ($35\mathrm{CO_2}+t\mathrm{Cl}$), the cubes were removed from the carbonation chamber, vacuum saturated using deionised water, rewrapped in vinyl tape, and placed in a sealed container with 3% sodium chloride solution. After the desired length of time, the cubes were removed from solution, unwrapped, oven dried at 30 °C for 1 h, and then split open to reveal internal material.

When measuring the chloride penetration depth in previously carbonated specimens using silver nitrate, studies [42] suggest that reactions between the silver nitrate solution and carbon trioxide (CO_3) can result in a whitish colour on the surface of the concrete [42] that may lead to false positive results in the measurement of the chloride front. In the current work, false positives were indeed observed when split surfaces of previously carbonated specimens were sprayed solely with 0.1 mol/L silver nitrate solution. To mitigate these effects, the approach of Pontes et al. [43] was therefore applied: after splitting, one of the freshly split surfaces was sprayed with saturated sodium hydroxide solution at a concentration of 150 g/L, placed in the oven at 30 °C for 1 h, and then sprayed twice with 0.1 mol/L silver nitrate solution. However, one repercussion was that the application of sodium hydroxide appeared to reduce the clarity of the colour change at the chloride front. There is, therefore, more uncertainty in these chloride penetration depth measurements.

2.7 Measurement of carbonation or chloride penetration depths

The penetration depths of the carbonation and chloride ingress fronts were measured on the split samples at 0, 7, 14 or 18, and 35 days. For each sample, five carbonation or silver nitrate chloride penetration depths were measured at regular intervals along the exposed face using vernier callipers. The overall penetration depth for each cube was calculated as the average of these five measurements, excluding measurements more than 10% away from the mean measurement as outliers.

Chloride penetration profiles were also determined in accordance with BS EN 14629:2007 [44]. A pillar drill was used to extract ground powder over depth increments of 5 mm after chloride exposure. This was

done at depths of 5–10 mm, 10–15 mm, 15–20 mm, 20–25 mm and 25–30 mm. The initial surface chloride content, C_0, was also measured from samples drilled at 0–5 mm depth prior to any chloride exposure. All samples were taken from locations at least 10 mm from the cube edges to mitigate any influence from transverse chloride diffusion through the side faces. The ground samples were passed through a 250 µm sieve, to remove large pieces of aggregate, and stored in airtight conditions prior to testing. The acid-soluble chloride content of each ground sample was then determined using a Rapid Chloride Test system.

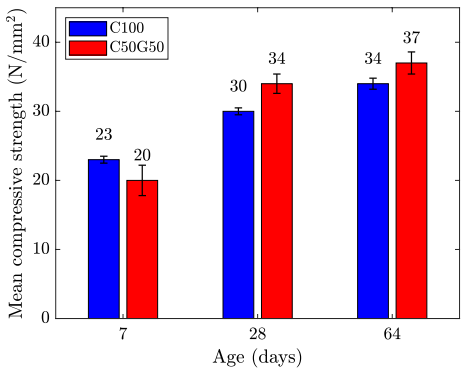

Fig. 1 Compressive cube strengths for C100 and C50G50 cubes. Error bars indicate one standard deviation

3 Experimental results and analysis

3.1 Compressive strength results

As shown in Fig. 1, at 7 days, the average compressive cube strength of C100 was greater than that of C50G50 but at 28 and 64 days, C50G50 had a higher average strength than that of C100. Cement replacement with GGBS has been found elsewhere [45] to lead to a slower early age strength development. The strengths of the two mixes were broadly similar over the timeframes under consideration.

3.2 Carbonation as single exposure ($35+t\mathrm{CO_2}$), and with prior chloride ingress ($35\mathrm{Cl}+t\mathrm{CO_2}$)

Figure 2 shows the carbonation fronts revealed by Ph indication for C100 and C50G50, measured throughout phase 2 carbonation exposure with or without prior chloride ingress. Despite five of the sides being covered with vinyl tape, there is some unintentional carbonation on the taped sides, showing the sealing was not fully effective. A small amount of initial carbonation is observed only in the C50G50 single exposure specimen, which remained for 35 days in sealed conditions during phase 1 ($35+0\mathrm{CO_2}$). For all other combinations, the initial carbonation depth, x_0, is zero.

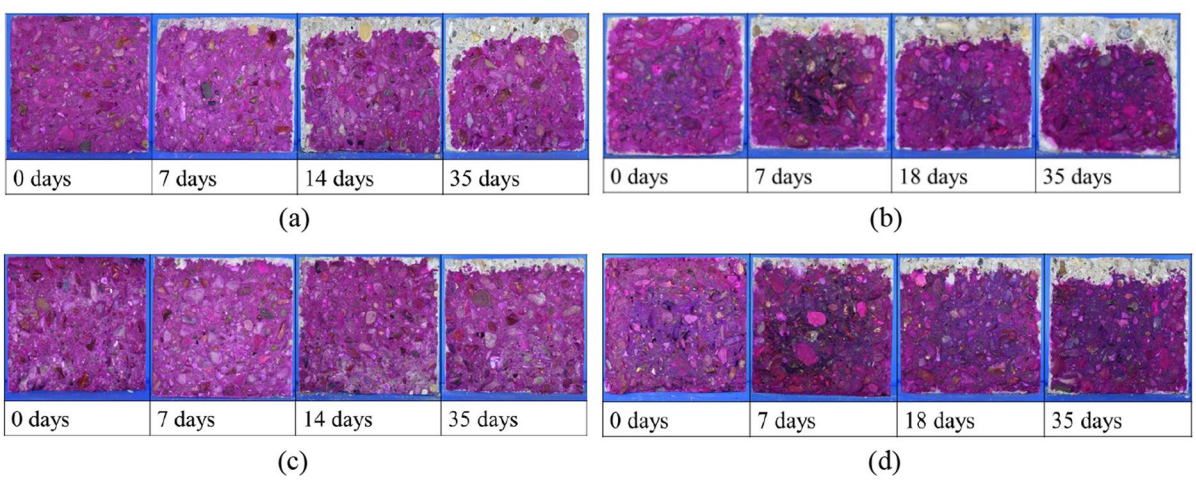

Fig. 2 Carbonation fronts for **a** C100 under single exposure: $35+t\mathrm{CO_2}$ **b** C50G50 under single exposure: $35+t\mathrm{CO_2}$ **c** C100 under dual exposure with prior chloride ingress $35\mathrm{Cl}+t\mathrm{CO_2}$ **d** C50G50 under dual exposure with prior chloride ingress $35\mathrm{Cl}+t\mathrm{CO_2}$

Various models have been presented for carbonation within concrete elements [46] [47] [48]. Diffusion-controlled carbonation is derived using Fick's first law, where the carbonation depth, x_{CO_2}, is proportional to the square root of time, t [49]. If an initial carbonated depth, x_o, is present at the start of the measured time interval, this influence can be modelled using a non-linear approach [50], where:

$$x_{CO_2} = \sqrt{x_o^2 + K_{CO_2}^2 t} \quad (1)$$

and K_{CO_2} is the carbonation coefficient.

The measured carbonation depths are plotted against the square root of time in Fig. 3. Best-fit lines indicate that the fit of Eq. 1 to the data produces R^2 values greater than 0.92, suggesting good agreement with Fick's first law [49]. The gradients of the best-fit lines are equal to the carbonation coefficients, K_{CO_2}, in specimens where $x_0 = 0$, and tend towards this value when using the non-linear approach from [50] to account for a non-zero initial carbonation depth. The K_{CO_2} results are summarised in Table 3.

The coefficients in Table 3 show that, for both concrete mixes investigated here, specimens which underwent dual exposure with chloride ingress prior to accelerated carbonation ($35Cl + tCO_2$) had lower carbonation rates than specimens which underwent single exposure ($35 + tCO_2$). The apparent reduction in coefficient due to dual exposure is larger in C100 (−58%) than C50G50 (−39%). The C50G50 specimens exhibited a larger carbonation coefficient than C100 under either single or dual exposure conditions.

Table 3 Carbonation coefficients (K_{CO_2}) for carbonation with and without prior chloride ingress for C100, C50G50

	K_{CO_2} (mm/day$^{1/2}$)	
	$35 + tCO_2$	$35Cl + tCO_2$
C100	2.95	1.25
C50G50	4.21	2.56

3.3 Chloride ingress as single exposure ($35 + tCl$), and with prior carbonation ($35CO_2 + tCl$)

Figure 4 shows the chloride ingress fronts from silver nitrate indication for C100 and C50G50, measured throughout phase 2 chloride exposure with or without prior carbonation. There is some unintentional chloride ingress through the sealed sides of the cubes indicating imperfect sealing.

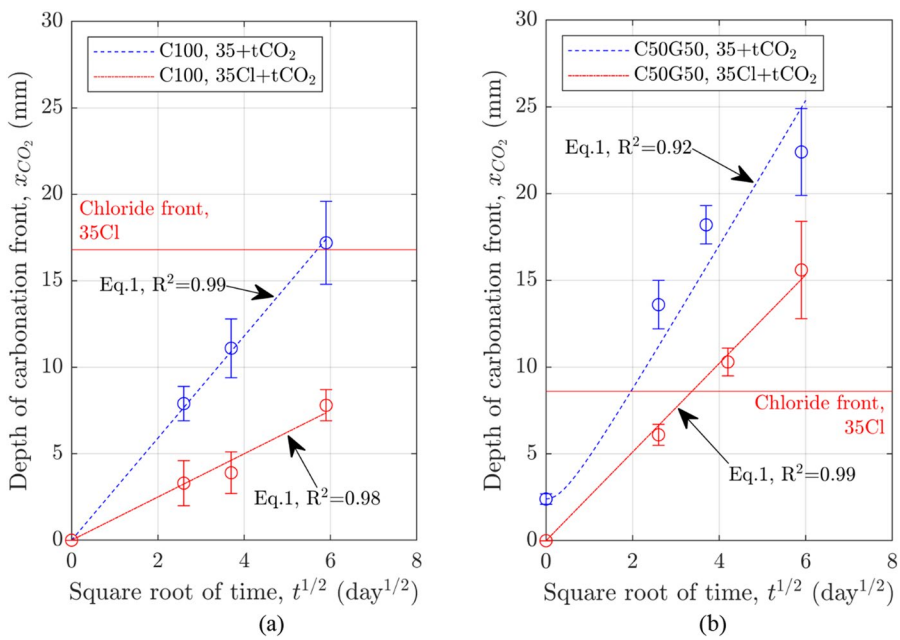

Fig. 3 Depth of the carbonation front against the square root of time for carbonation with and without prior chloride ingress for **a** C100 and **b** C50G50. Error bars indicate one standard deviation in measurements

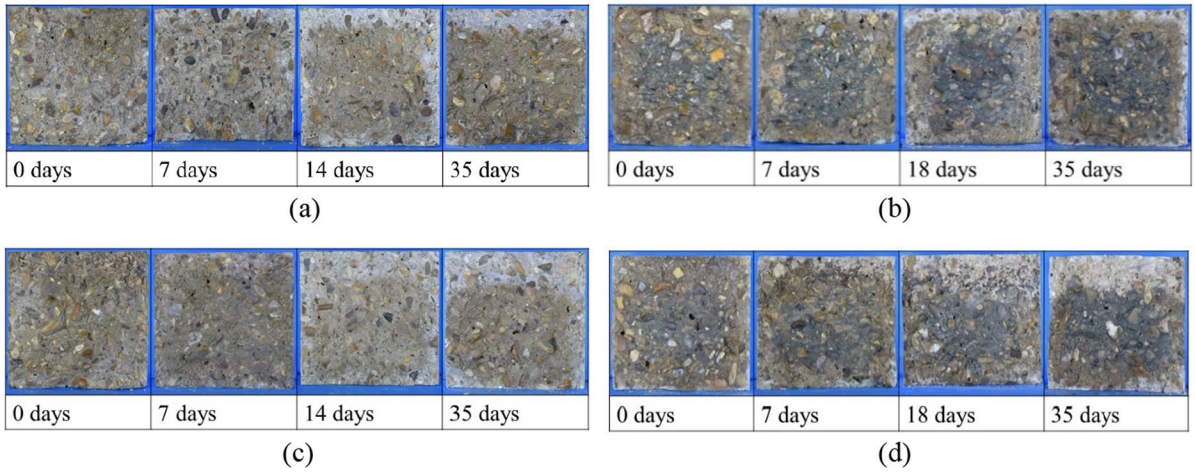

Fig. 4 Chloride penetration for (**a**) C100 under single exposure: 35 + *t*Cl (**b**) C50G50 under single exposure: 35 + *t*Cl (**c**) C100 under dual exposure with prior carbonation 35CO_2 + *t*Cl (**d**) C50G50 under dual exposure with prior carbonation 35CO_2 + *t*Cl

The chloride concentration inside concrete is typically modelled using Fick's second law of diffusion [51]:

$$C(x,t) = C_0 + C_s\left[1 - \mathrm{erf}\left(\frac{x}{2\sqrt{D_{Cl}t}}\right)\right] \quad (2)$$

where C is the chloride content at depth x at time t, C_0 is the initial chloride content prior to chloride exposure, C_s is the chloride content at the surface, D_{Cl} is the chloride diffusion coefficient and erf is the error function. As a result, the penetration depth of the critical chloride content, x_{Cl}, is proportional to the chloride diffusion coefficient, K_{Cl} and the square root of exposure time, t, [46]:

$$x_{Cl} = K_{Cl}\sqrt{t} \quad (3)$$

assuming constant diffusion coefficients and surface chloride contents. In reality, these parameters are strongly time dependent [52].

The measured chloride ingress fronts are plotted against the square root of time in Fig. 5. The chloride coefficients, K_{Cl} [46], calculated based on the best fit of Eq. 3 to the chloride front measurements obtained by the silver nitrate test, are presented in Table 4. The best-fit lines have R^2 values greater than or equal to 0.80, indicating reasonably good fit with Fickian diffusion model. However, is noted that Eq. 3 does not fit the chloride ingress data as well as Eq. 1 fits the carbonation results. This indicates that there are some time dependencies in the chloride coefficient which are not observed in the carbonation coefficient.

Due to the concerns about the less distinct visual front in the samples with prior carbonation, seen in Fig. 4, RCT measurements were also taken. In Fig. 6, the RCT derived acid soluble chloride contents at different depths are presented. The depth was plotted as the mid-point of the range under consideration e.g. powder from 5–10 mm was noted as 7.5 mm. The measured location of the carbonation front at 35 days (denoted as 'Ph carbonation front, 35 CO_2') is also shown.

Using the initial chloride content prior to chloride exposure C_0, the surface chloride content C_S and the chloride diffusion coefficient D_{Cl} were both back-calculated from the measured acid-soluble chloride contents in Fig. 6, by fitting Eq. 2 to the data using non-linear-least-squares optimisation. These results are also presented in Table 4.

The chloride coefficients,K_{Cl}, presented in Table 4 suggest that dual exposure with prior carbonation (35CO_2 + 35Cl) increased the rate of chloride penetration in both concrete mixes when compared to single exposure to chloride ingress (35 + 35Cl). With a caveat about the quality of the fit, the inclusion of slag led to a greater increase in K_{Cl}, + 135% for C50G50 versus + 66% for C100, due to prior carbonation. The RCT results in Fig. 6 further show that,

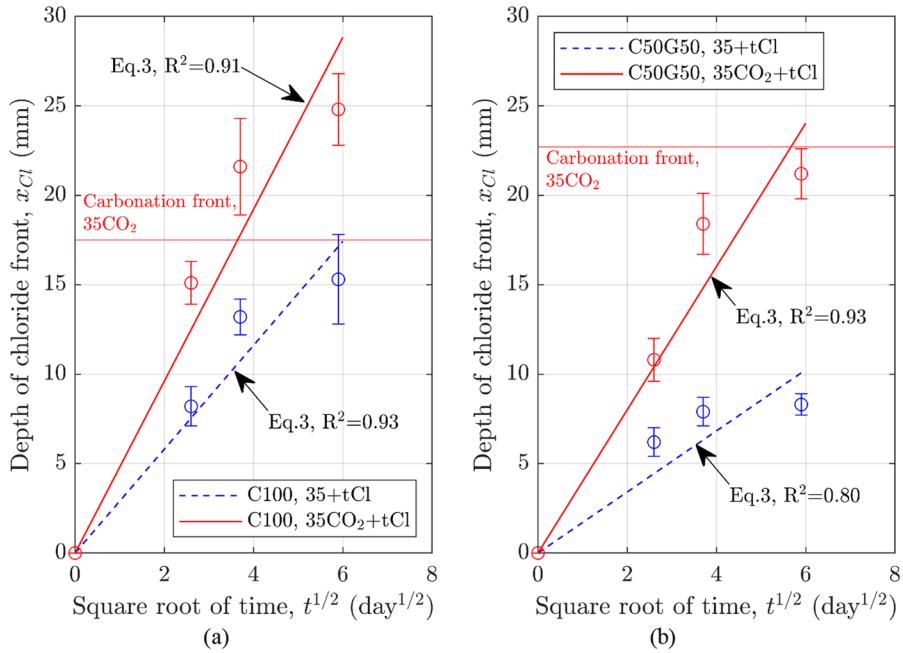

Fig. 5 Depth of the chloride ingress front against the square root of time for chloride ingress with and without prior carbonation for **a** C100 and **b** C50G50. Error bars indicate one standard deviation in measurements

Table 4 Chloride coefficient, (K_{Cl}), initial chloride content prior to chloride exposure (C_0), surface chloride content (C_S) and diffusion coefficient (D_{Cl}) for chloride ingress without and with prior carbonation

		K_{Cl} (mm/day$^{1/2}$)	C_0 (%)	C_S (%)	D_{Cl} (mm^2/day)
C100	35 + 35Cl	2.90	0.001	0.24	2.41
	35CO$_2$ + 35Cl	4.81	0.005	0.11	43.65
C50G50	35 + 35Cl	1.70	0.009	0.34	0.75
	35CO$_2$ + 35Cl	4.00	0.011	0.07	45.18

with the exception of the readings at 7.5 mm, the chloride contents in the previously carbonated specimens (35CO$_2$ + tCl) appear to be similar or higher than those with no prior carbonation (35 + tCl). The acid-soluble chloride contents in the C50G50 samples were generally lower than those in the C100 samples at any given depth. Whereas Eq. 2 showed a good fit for single exposure to chloride ingress (35 + tCl, $R^2 > 0.98$), the correlation for dual exposure with prior chloride ingress was relatively poor (35CO$_2$ + tCl, $R^2 < 0.19$). This appears to be in part due to a higher acid-soluble chloride content in the region of the carbonation front and will be discussed further in the next section.

4 Discussion

4.1 Carbonation with prior chloride ingress

The carbonation coefficients under dual exposure with prior chloride ingress were 58% and 39% smaller than the carbonation coefficients under single exposure, for C100 and C50G50 respectively.

The observed reduction in carbonation rate for the concretes exposed to prior chloride ingress could be due to changes in pore structure. Prior chloride exposure has been found to reduce the total porosity and the proportion of medium and large capillary pores in OPC concretes [21, 23] and the reduction in total porosity is felt to be due, in part, to salt physically blocking the pores of the cement matrix, consequently hindering the penetration of CO_2 [22, 23] The hygroscopic nature of salt has also been proposed

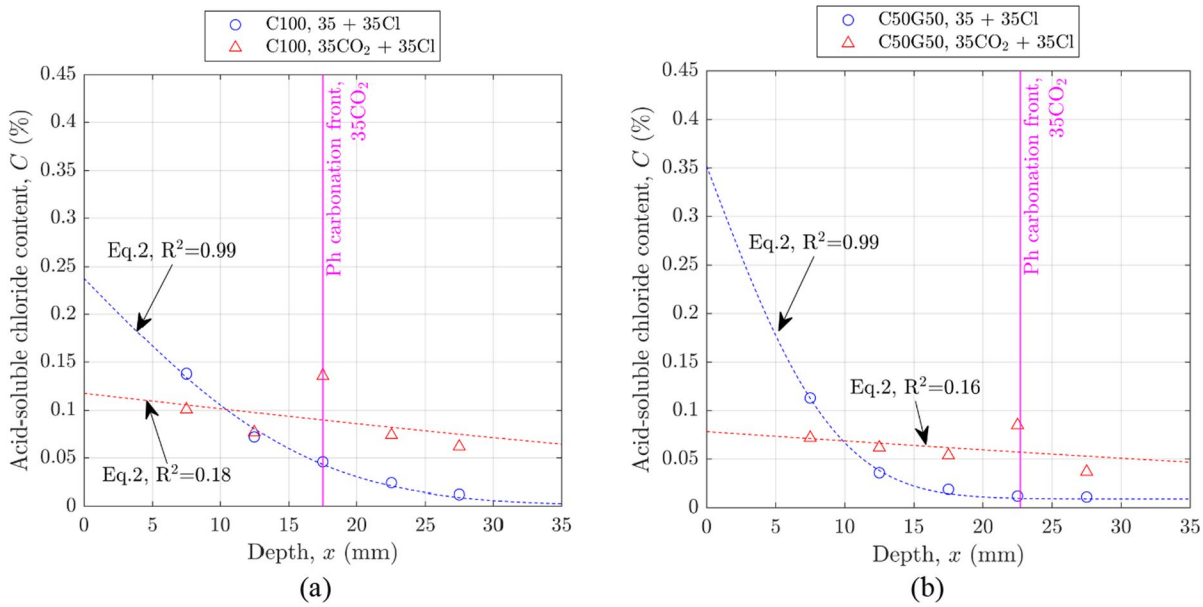

Fig. 6 Chloride penetration profiles for chloride ingress with and without prior carbonation at 35 days for **a** C100 and **b** C50G50 with 35 day Phenolphthalein (Ph) front noted

as a factor in reducing carbonation in OPC mortars [22]. It appears that the resistance of C100 to carbonation is more affected by prior chloride ingress than that of C50G50. Under single exposure chloride ingress, GGBS replacement has been found to reduce rates of chloride ingress relative to OPC, due to the refined pore structure and improved chloride binding capacity of cement pastes with GGBS replacement as a result of the increased aluminate content of GGBS [17, 24, 28, 29].

Figure 3 suggests that for C100, the carbonation front has not yet reached the depth of chloride penetration associated with the initial period of immersion, whereas, for C50G50, the carbonation depth has progressed beyond the depth of prior chloride ingress. It might be expected that the carbonation rate thereafter would approach that of the concrete without prior chloride ingress. Unfortunately, the large variation in the C50G50 observed carbonation depth at 35 days, resulting in large error bars on this data point, makes it difficult to reach definitive conclusions.

Since the C50G50 sequential exposure carbonation coefficient was back-calculated using data within and beyond the chloride front, this could therefore underestimate the relative reduction in carbonation coefficient due to prior chloride ingress and contribute to a smaller difference between the single and dual exposure carbonation coefficients relative to the OPC specimens where the carbonation front remained within the prior chloride front.

Chloride redistribution has been observed elsewhere when cement pastes are exposed to prior chloride ingress and then carbonation [18, 20] and so one point of note is that the chloride ingress front measured using silver nitrate solution may be less accurate. Nevertheless, based on the results reported here (see Fig. 3), carbonation through concrete previously exposed to chloride ingress appears to be fairly accurately modelled using Fick's first law.

4.2 Chloride ingress with prior carbonation

Prior carbonation increased the rate of chloride ingress in both concrete mixes, which is consistent with findings elsewhere [4, 14, 15]. For C100 and C50G50, the diffusion coefficients, D_{Cl}, were significantly greater and the chloride coefficients, K_{Cl}, under dual exposure with prior carbonation were respectively 66 or 135% larger than those under single exposure. The surface chloride content, C_S, was lower in specimens with prior carbonation (see Table 4). In

Fig. 5, the C100 chloride front reaches depths greater than the prior carbonation front whereas the C50G50 chloride front remains within carbonated material. Hence the C100 back-calculated chloride coefficient includes progression through both carbonated and non-carbonated material. This potentially underestimates the relative increase in chloride coefficient due to prior carbonation.

The observed increases in the chloride coefficient for concrete exposed to prior carbonation are potentially due to changes in the pore structure and chloride binding capacity of concrete that has undergone carbonation. Contributing factors could be an increase in the proportion of large capillary pores, due to the decomposition of C–S–H gel [17], carbonation-induced microcracking [9], a reduction in the chloride binding capacity due to AFm phase reactions with carbonate ions, which deplete the AFm availability for reactions with chloride ions to form Friedel's salt [18], and the reduced pH value of concrete pore solution due to carbonation, which increases the solubility of Friedel's salt [20]. Notwithstanding the previous caveat about C100 chloride progression into non-carbonated concrete, it appears that the resistance of C50G50 to chloride ingress is more affected by prior carbonation than that of C100. Under single exposure carbonation, an increased carbonation rate due to GGBS replacement [27–29] is attributed to the consumption of portlandite during the hydration of GGBS, lowering the alkalinity of the cement paste [27]. In addition, Ngala and Page found that the increase in capillary porosity and in the proportion of large capillary pores due to carbonation is greater for pastes containing GGBS than for OPC pastes [17]. Therefore, the larger extent of carbonation in C50G50 compared to C100 could explain why the chloride coefficient of C50G50 is more affected by carbonation than that of C100.

Changes in the pore structure and chloride binding capacity due to prior carbonation also contribute to explaining the shape of the acid soluble chloride profiles observed in this study. Figure 6 shows that Eq. 2 was a relatively poor fit for the specimens with prior carbonation ($35CO_2 + 35Cl$). For both mixes, an uplift in acid soluble chloride content observed at a depth approximately coincident with the phenolphthalein indicated carbonation depth was not captured with a continuous error function curve. This also suggested that the equivalent surface concentration for the non-carbonated material was higher than for the carbonated material. To investigate further, Eq. 2 was fitted separately to the acid soluble chloride contents

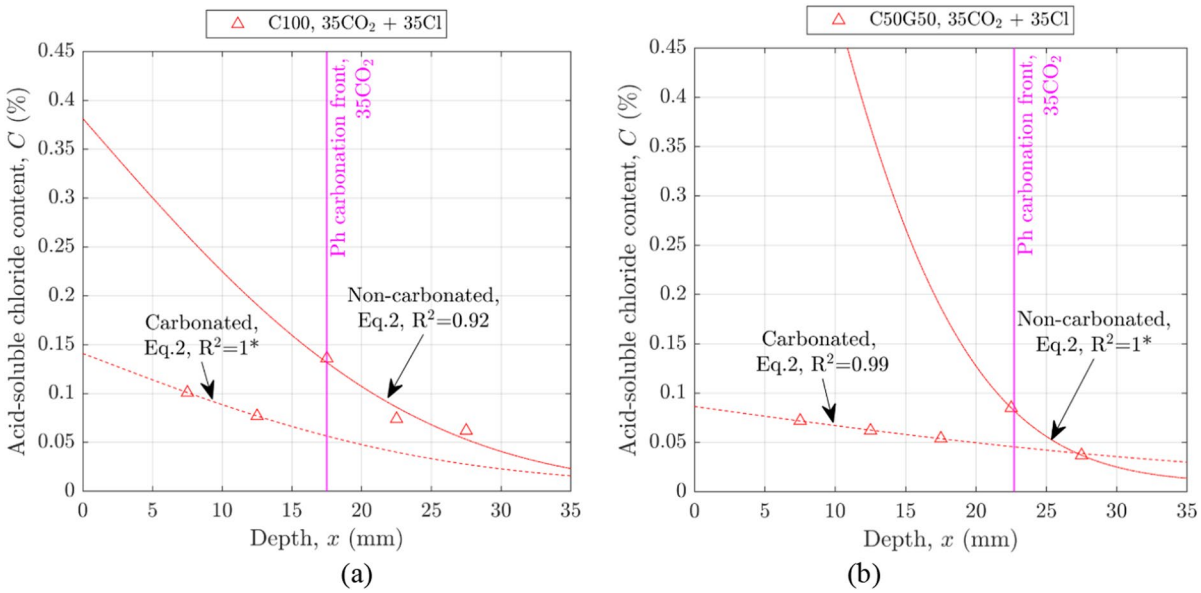

Fig. 7 Curve fitting in carbonated and non-carbonated regions of the chloride penetration profiles of **a** C100 and **b** C50G50 for the case of carbonation followed by chloride exposure ($35CO_2 + 35Cl$). *Note that an R^2 value of 1 is inevitable when a fit is generated with only two datapoints, and therefore does not necessarily indicate a high quality of fit

Table 5 Chloride ingress parameters in specimens with prior carbonation treating carbonated and non-carbonated regions separately

			C_0 (%)	C_S (%)	D_{Cl} (mm^2/day)
C100	$35CO_2+35Cl$	Carbonated region	0.005	0.14	5.65
		Non-carbonated region	0.001*	0.38	4.88
C50G50	$35CO_2+35Cl$	Carbonated region	0.011	0.08	13.34
		Non-carbonated region	0.009*	1.19	2.11

*Inferred from measurements taken on non-carbonated specimens

before and after the carbonation front, as shown in Fig. 7. The associated surface chloride contents in the non-carbonated (free face) and carbonated (from the interior side of the carbonation front) regions and the chloride diffusion coefficients are indicated in Table 5.

Ye et al. [20] also found a similar drop in chloride content at the surface and a maximum chloride content that appeared to coincide with the carbonation front when investigating chloride ingress in concrete exposed to cyclic drying-wetting and carbonation. This was attributed to an increase in the solubility of Friedel's salt due to a carbonation-induced reduction in the concrete pore pH resulting in a chloride gradient that increases the inward movement of chloride ions [20]. A higher proportion of large capillary pores and microcracking near the surface of the carbonated zone would also contribute to an inward movement of chloride ions in the carbonated zone [9]. A combination of changes in the solubility of Friedel's salt and the permeability of samples at the interface between the carbonated and non-carbonated zones might therefore explain the build-up of chloride ions at the interface, leading to the observed increase in the acid-soluble chloride content in the boundary region.

Zhu et al. [13] differentiated between carbonated and non-carbonated zones when modelling the simultaneous combined action of carbonation and chloride ingress. They proposed that the chloride content increases up to the carbonation boundary and then decays through the non-carbonated region, in both cases following error functions [13]. The chloride content at the carbonation front interface was used as a common boundary condition for the non-carbonated and carbonated regions. However, the sequential exposure experimental findings presented here suggest that the chloride content is decreasing from the free face through the carbonated region and then increases adjacent to the carbonation front. Although further data supported with microstructural and compositional analyses would be required for more definitive conclusions, this suggests that caution should be exercised when using a continuous Fickian function to model chloride ingress in OPC or OPC/GGBS concrete specimens exposed to prior carbonation. Initial chloride content measurements taken close to the surface could lead to the calculation of a chloride diffusion coefficient that underestimates the chloride content at the depth of the steel reinforcement. The initial findings suggest that a piece-wise model could hold promise.

4.3 Limitations, practical implications and future work

The results show that the sequence of carbonation or chloride ingress affects the ingress of these chemicals into OPC and OPC/GGBS concrete. Sequential exposure suits laboratory environments and can be performed under controlled conditions but in practice CO_2 and Cl exposure often occurs simultaneously rather than in sequence. In the current work, chloride exposure was invoked using full immersion in salt solution [33] with a concentration similar to sea water, whereas concrete in tidal zones would be wetting and drying due to submersion at high tide and exposure to air at low tide. The moisture content of the concrete has implications for the rate of CO_2 or Cl penetration and, in particular, the humidity content has been found to affect the rate of carbonation [53]. To provide a repeatable methodology, the experimental specimens were subjected to air curing for a set period (for CO_2 penetration) or vacuum saturation with deionised water for Cl penetration (with or without prior carbonation). The humidity in the CO_2 chamber was also controlled. However, the internal moisture conditions for single exposure to CO_2 were likely to differ from those after a period of oven and

air drying in the sequential exposure tests with prior Cl immersion.

The extended timeframes for measurable ingress using natural CO_2 concentrations can be prohibitive for typical research investigations or for practical mix characterisation so an elevated CO_2 concentration was used to accelerate ingress. However, this can impact different mix compositions in different ways. The relatively high *w/b* ratio used in the experimental mixes was also driven by a desire for rapid ingress such that compositional differences could be observed. The consequence of these choices meant that the prior carbonation front had extended relatively deep into the concrete (> 15 mm) prior to chloride exposure which would not have been the case with natural carbonation and/or a mix with a low *w/b* ratio. The current study kept the sequential exposure conditions the same for the C100 and C50G50 mixes. Hence the depth of the prior chloride or carbonation front at the time of subsequent dual exposure differed since the two mixes had different resistances. Future testing of samples with different prior exposure times, and the acquisition of more data at smaller time intervals would help to capture progression before, through and beyond a prior carbonation or prior chloride front. In this way the behaviour in these regions could be better interrogated. Further work is also required to translate and quantify the implications for design applications and concrete mixes used in practice. Nevertheless, the sequential exposure studies conducted here suggest that differences between mixes could be identified and so the approach could potentially provide the basis for short-term accelerated characterisation to inform concrete mix design and mix selection for onerous durability design conditions.

5 Conclusions

In practical applications, concrete structures can be exposed to both carbonation and chloride ingress, either simultaneously or in succession. An experimental investigation was undertaken to better understand the impact of prior carbonation on chloride ingress and vice versa, and the implications for a cementitious binder with or without 50% GGBS cement replacement. For carbonation, specimens were exposed to an accelerated environment of 10% CO_2 concentration for up to 35 days. For chloride ingress, specimens were immersed in 3% sodium chloride solution for up to 35 days.

- In dual exposure, specimens subjected to prior chloride ingress followed by carbonation showed a decreased carbonation rate in both the concrete containing GGBS and that without, when compared to specimens without prior chloride ingress. The apparent reduction in carbonation coefficient due to dual exposure was larger in C100 than C50G50.
- Specimens of both concrete mixes subjected to dual exposure with prior carbonation followed by chloride ingress showed an increased rate of chloride ingress when compared to specimens without prior carbonation exposure. The increase in the chloride coefficient due to prior carbonation was greater in C50G50 than C100.
- The back-calculation of a single carbonation or a single chloride diffusion coefficient for cases where carbonation passes through a prior chloride front, or chloride passes beyond a prior carbonation front may mask progression rate differences before and after the front.
- Acid soluble penetration profiles for chloride ingress with prior carbonation do not appear to follow a continuous Fickian diffusion error function curve. Hence, modelling of chloride ingress with prior carbonation using a continuous function and initial chloride content measurements close to the surface could lead to an underestimate of the free chloride content at the depth of the steel reinforcement.

Acknowledgements The authors (JML/JCF) gratefully acknowledge the support of the UK Engineering and Physical Sciences Research Council through grants EP/N017668/1—Tailored Reinforced Concrete Infrastructure and EP/N509620/1—University of Cambridge Doctoral Training Partnership. The technical support from staff in the University of Cambridge Civil Engineering Research Laboratories, and use of the Civil Engineering and EPSRC UKCRIC National Research Facility for Infrastructure Sensing (EP/P013848/1) experimental facilities (EP/P013848/1) is also much appreciated.

Author contribution Grace Blackshaw Conceptualization; Methodology; Software; Validation; Formal analysis; Investigation; Data Curation; Writing—Original Draft; Writing—Review & Editing; Visualization. Jessica C. Forsdyke Conceptualization; Software; Formal analysis; Resources;

Writing—Review & Editing; Visualization; Supervision; Project administration. Janet M. Lees Conceptualization; Resources; Writing—Review & Editing Preparation; Supervision; Project administration; Funding acquisition. For the purpose of open access, the authors have applied a Creative Commons Attribution (CC BY) licence to any Author Accepted Manuscript version arising.

Funding Engineering and Physical Sciences Research Council, EP/N017668/1, Janet M. Lees, EP/N509620/1, Jessica C. Forsdyke, EP/P013848/1.

References

1. Hansson CM (1995) Concrete: the advanced industrial material of the 21st century. Metall and Mater Trans A 26:1321–1341
2. Balafas I, Burgoyne CJ (2011) Modelling the structural effects of rust in concrete cover. J Eng Mech 137(3):175–185
3. Angst U, Elsener B, Jamali A, Adey B (2012) Concrete cover cracking owing to reinforcement corrosion—theoretical considerations and practical experience. Mater Corros 63(12):1069–1077
4. Li K, Zhang Y, Wang S, Zeng J (2018) Impact of carbonation on the chloride diffusivity in concrete: experiment, analysis and application. Mater Struct 51(6):164
5. Kim YY, Lee KM, Bang JW, Kwon SJ (2014) Effect of W/C ratio on durability and porosity in cement mortar with constant cement amount. Adv Mater Sci Eng 2014:1–11
6. British Standards Institution (2015) BS 8500-1:2015+A2:2019, Concrete-Complementary British Standard to BS EN 206-1; Part 1: Method of specifying and guidance for the specifier
7. Karri SK, Rao GVR, Raju PM (2015) Strength and durability studies on GGBS concrete. SSRG Int J Civ Eng 2(10):34–41
8. Cyr M (2013) Influence of supplementary cementitious materials (SCMs) on concrete durability. Eco-Efficient Concrete. Elsevier, Amsterdam, pp 153–197
9. Wang Y, Nanukuttan S, Bai Y, Basheet PAM (2017) Influence of combined carbonation and chloride ingress regimes on rate of ingress and redistribution of chlorides in concretes. Constr Build Mater 140:173–183
10. Kuosa H, Ferreira RM, Holt E, Leivo M, Vesikari E (2014) Effect of coupled deterioration by freeze-thaw, carbonation and chlorides on concrete service life. Cement Concr Compos 47:32–40
11. Zhu X, Zi G, Cao Z, Cheng X (2016) Combined effect of carbonation and chloride ingress in concrete. Constr Build Mater 110:369–380
12. Zhu X, Zi G, Sun L, You I (2019) A simplified probablistic model for the combined action of carbonation and chloride ingress. Mag Concr Res 71(7):327–340
13. Zhu X, Dai X, Liu L, Bian W, Xu L, Meng Z (2020) A simplified coupling model of carbonation and chloride ingress based on Stefan-like condition. Eur J Environ Civ Eng 26(7):2654–2670
14. Al-Ameeri AS, Rafiq MI, Tsioulou O (2021) Combined impact of carbonation and crack width on the chloride penetration and corrosion resistance of concrete structures. Cem Concr Compos 115:103819
15. Li K, Zhao F, Zhang Y (2019) Influence of carbonation on the chloride ingress into concrete: theoretical analysis and application to durability design. Cem Concr Res 123:105788
16. Malheiro R, Camoes A, Meira G, Amorim MT, Castro-Gomes J (2020) Interaction of carbonation and chloride ions ingress in concrete. RILEM Tech Lett 5:56–62
17. Ngala VT, Page CL (1997) Effects of carbonation on pore structure and diffusional properties of hydrated cement pastes. Cem Concr Res 27(7):995–1007
18. Chang H (2017) Chloride binding capacity of pastes influences by carbonation under three conditions. Cement Concr Compos 84:1–9
19. Matschei T, Lothenbach B, Glasser F (2007) The AFm phase in Portland cement. Cem Concr Res 37(2):118–130
20. Ye H, Jin X, Fu C, Jin N, Xu Y, Huang T (2016) Chloride penetration in concrete exposed to cyclic drying-wetting and carbonation. Constr Build Mater 112:457–463
21. Liu J, Qui Q, Chen X, Xing F, Han N, He Y, Ma Y (2017) Understanding the interacted mechanism between carbonation and chloride aerosol attack in ordinary Portland cement concrete. Cem Concr Res 95:217–225
22. Malheiro R, Camoes A, Ferreira RM, Meira G, Amorim T, Rei R (2014) Carbonation front progress in mortars containing fly ash considering the presence of chloride ions. Key Eng Mater 634:214–221
23. Malheiro R, Camoes A, Gibson M, Maria Teresa A (2021) Influence of chloride contamination on carbonation of cement-based materials. Constr Build Mater 296:123756
24. Black L (2016) Low clinker cement as a sustainable construction material. Sustainability of construction materials. Elsevier Ltd., Amsterdam, pp 415–457
25. Bouikni A, Swarmy RN, Bali A (2009) Durability properties of concrete containing 50% and 65% slag. Constr Build Mater 23:2836–2845
26. Papadakis V (2000) Effect of supplementary cementing materials on concrete resistance against carbonation and chloride ingress. Cem Concr Res 30:291–299
27. Gruyeart E, Van den Heede P, De Belie N (2013) Carbonation of slag concrete: effect of the cement replacement

level and curing on the carbonation coefficient. Cement Concr Compos 35(1):39–48
28. Elahi A, Basheer PAM, Nanukuttan SV, Khan QUV (2010) Mechanical durability properties of high-performance concretes containing supplementary cementitious materials. Constr Build Mater 24(3):292–299
29. Dhir RK, El-Mohr M, Dyer TD (1996) Chloride binding in GGBS concrete. Cem Concr Res 26:1767–1773
30. Abd El-Fattah H, Abd El-Zaher Y, Kohail M (2024) A study of chloride binding capacity of concrete containing supplementary cementitious materials. Sci Rep 14:12970
31. De Weerdt K (2021) Chloride binding in concrete: recent investigations and recognised knowledge gaps. Mater Struct 54:214
32. Van den Heede P, De Schepper M, De Belie N (2019) Accelerated and natural carbonation of concrete with high volumes of fly ash: chemical, mineralogical and microstructural effects. Royal Soc Open Sc 6(1):18665
33. British Standards Institution (2015) BS EN 12390-11:2015 Testing hardened concrete. Determination of the chloride resistance of concrete, unidirectional diffusion
34. Neves R, Branco F, de Brito J (2013) Field assessment of the relationship between natural and accelerated concrete carbonation resistance. Cem Concr Compos 41:9–15
35. Cui H, Tang W, Liu W, Dong Z, Xing F (2015) Experimental study on effects of CO_2 concentrations on concrete carbonation and diffusion mechanisms. Constr Build Mater 93:522–527
36. Teychenne DC, Franklin RE, Erntroy HC, Marsh BK (1997) Design of Normal Concrete Mixes. Building Research Establishment, Watford
37. Higgins D (2009) Portland cement replacement: within-mixer or factory-blend? Ready-Mix Concr 23:22–24
38. Oner A, Akyuz S (2007) An experimental study on optimum usage of GGBS for the compressive strength of concrete. Cem Concr Compos 29(6):505–514
39. British Standards Institution (2019) BS EN 12390-2:2019 Testing hardened concrete. Making and curing specimens for strength tests
40. British Standards Institution (2019) BS EN 12390-3:2019 Testing hardened concrete. Compressive strength of test specimens
41. Chinchon-Paya S, Andrade C, Chinchon S (2016) Indicator of carbonation front in concrete as substitute to phenolphthalein. Cem Concr Res 82:87–91
42. Real LV, Oliveira DRB, Soares T, Medeiros MHF (2015) $AgNO_3$ spray method for measurement of chloride penetration: state of the art. ALCONPAT J 5(2):141–151
43. Pontes CV, Reus GC, Araujo EC, Medeiros MHF (2021) Silver nitrate colorimetric method to detect chloride penetration in carbonated concrete: how to prevent false positives. J Build Eng 34:101860
44. British Standards Institution (2007) BS EN 14629:2007 Products and systems for the protection and repair of concrete structures—test methods—determination of chloride content in hardened concrete
45. Suresh D, Nagaraju K (2015) Ground granulated blast slag (GGBS) in concrete—a review. IOSR J Mech Civil Eng 12(4):76–82
46. Zhou Y, Gencturk B, William K, Attar A (2015) Carbonation-induced and chloride-induced corrosion in reinforced concrete structures. J Mater Civ Eng 27(9):04014245
47. Qiu Q (2020) A state-of-the-art review on the carbonation process in cementitious materials: Fundamentals and characterization techniques. Constr Build Mater 247:118503
48. Czarnecki L, Woyciechowski P (2015) Modelling of concrete carbonation; Is it a process unlimited in time and restricted in space? Bull Polish Acad Sci: Tech Sci 63(1):43–54
49. Kropp J, Hilsdorf HK (1995) Performance criteria for concrete durability, RILEM. CRC Press, Boca Raton
50. Forsdyke JC, Lees JM (2023) Model fitting to concrete carbonation data with non-zero initial carbonation depth. Mater Struct 56:22
51. Costa A, Appleton J (1999) Chloride penetration into concete in marine environment—Part I: Main parameters affecting chloride penetration. Mater Struct 32(4):252–259
52. Yu H, Tan Y, Feng T (2019) Study of temporal change in chloride diffusion coefficient of concrete. ACI Mater J 116:103–112
53. Xu Z, Zhang Z, Huang J, Yu K, Zhong G, Chen F, Chen X, Yang W, Wang Y (2022) Effects of temperature, humidity and CO_2 concentration on carbonation of cement-based materials: a review. Constr Build Mater 346:128399